**Article publicat / Published article:**

Mohammadi, M. (2016) A new approach to design an efficient micropost array for enhanced direct-current insulator-based dielectrophoretic trapping. "Analytical and bioanalytical chemistry ". Vol. 408, issue 19, p.5285-5294. Doi: 10.1007/s00216-016-9629-2

# A new approach to design an efficient micropost array for enhanced direct-current insulator-based dielectrophoretic trapping

Mahdi Mohammadi[1, 2], Mohammad Javad Zare[3], Hojjat Madadi[4], Jasmina Casals-Terré*[2], Jordi Sellarès[2]

[1]Biomedical Diagnostics Institute, National Center for Sensor Research and School of Physics, Dublin City University, Dublin 9, Ireland

[2]Technical University of Catalonia, Mechanical Engineering Department, Terrassa, Spain

[3]Shiraz University, Mechanical Engineering Department, Shiraz, Iran

[4]Laboratory Colloïdes et Matériaux Divisés, ESPCI ParisTech, Paris 75005, France

# A new approach to design an efficient micropost array for enhanced direct-current insulator-based dielectrophoretic trapping

Mahdi Mohammadi[1, 2], Mohammad Javad Zare[3], Hojjat Madadi[4], Jasmina Casals-Terré*[2], Jordi Sellarès[2]

[1]Biomedical Diagnostics Institute, National Center for Sensor Research, Physics Dep, Dublin City University, Dublin 9, Ireland

[2]Technical University of Catalonia, Mechanical Engineering Department, Terrassa, Spain

[3]Shiraz University, Mechanical Engineering Department, Shiraz, Iran

[4]Laboratory Colloïdes et Matériaux Divisés, ESPCI ParisTech, Paris 75005, France

## Abstract

Direct-current insulator-based dielectrophoresis (DC-iDEP) is a well-known technique that benefits from the electric field gradients generated by an array of insulating posts to separate or trap biological particles. In this work, we propose a novel figure of merit to find an efficient design of the post-array distribution in a microfluidic channel. To maximize the particle trapping in the post-array, while minimizing the required voltage, with a similar footprint and channel thickness, a parametric numerical analysis has been done focusing on the geometric parameters of the post-array. It is found that the particle trapping condition along the central line of the transversal distance between posts can be defined as a new figure of merit to obtain an efficient design of the microposts array. Different post-array models with the variation of transversal distance (10 to 60 µm), longitudinal distance (10 to 80 µm) and post radius (10 to 150 µm) have been analyzed using COMSOL Multiphysics finite element software. The obtained results indicate that the radius post optimization allows the enhancement of the trapping condition between 56% (for a transversal distance of 10µm) up to 341% (for a transversal distance of 60µm). Based on the DC-iDEP numerical analysis on the microposts geometrical parameters for particle trapping maximization, we find out a new relationship between the optimum post radius and the transversal distance between the posts. According to the derived merit, the optimum post radius should be 40 µm more than the transversal distance between posts. For the validation of the numerical results, several microchannels with embedded post-arrays are manufactured in Polydimetilsiloxane (PDMS) and the particle trapping patterns of 6-µm-diameter polystyrene particles are measured experimentally. The experiments confirm the same trends as pointed out by the numerical analysis. The main advantage of these results is that they depend only on the geometry of the micropost array and are valid for trapping different particles suspended in different media. The results show that this new figure of merit and geometrical characterization can be used to reduce the required electric field to achieve effective particle trapping and, therefore, avoid the negative effects of Joule heating in cells or viable particles.

---

Mechanical Engineering Department- MicroTech Lab- BarcelonaTech University- Technical University of Catalonia -08222- Barcelona-Spain
E-mail. Jasmina.casals@upc.edu

**Abbreviation**

| | |
|---|---|
| DEP | Dielectrophoresis |
| DC | Direct current |
| EK | Electronkinetic |
| eDEP | Electrode based DEP |
| iDEP | Insulator based DEP |
| RBC | red blood cell |

## 1. INTRODUCTION

Lab-on-a-chip is a powerful tool in analytical chemistry and medical engineering. The lab-on-a-chip integrated with microfluidic systems enables miniaturization, integration, and automation of complex biochemical assays due to their advantages, including low requirements for samples and reagents, rapid operation, high convenience, and low cos [1].

Separation of cells or particles from a fluid is a vital step in many biochemical tests. Different microfluidic methods have been developed to this end (see review) [2-3]. Among these, the dielectrophoresis method (DEP) is a well-known technique to separate particles even in small sample volume [4].

Dielectrophoresis is a movement of particles caused by a polarization effect when a non-uniform electric field is applied to a channel with particles that have different conductivity than the medium. Since the dielectrophoretic force is proportional to the electric field gradient, it can appear either when direct current (DC) or alternate current (AC) is applied. The non-uniform electric field can be generated using an array of electrodes (electrode based, eDEP) [5-7] or an array of insulating posts (insulator based, iDEP).

The iDEP can overcome most of the well-known limitations of eDEP, taking advantage of the fact that in the case of iDEP the electric field gradient is achieved by changing the path track of the field using insulator obstacles rather than using complex shaped electrodes [8]. For instance, iDEP devices can provide a higher throughput since the technique is not limited to thin channels that confine the fluid on the electrode surface [9] and, moreover, most iDEP devices are able to produce an electroosmotic flow (EOF) eliminating the need of an external driving force [10-11].

In the other hand, the use of just two electrodes placed in the channel inlet and the channel outlet, offers other advantages such as a more straightforward fabrication process, less fouling than with embedded electrodes, minimum bubble generation inside the channel and less electrochemical reactions [12]. These devices are more appropriate for metal-sensitive organic samples. The iDEP microdevices including two separated electrodes in inlet and outlet have been successfully employed for different applications: separation and concentration of live and dead bacteria[13-14] separation of white blood cells [15], red blood cells (RBC) [16] or blood cell separation in a saw-tooth microchannel [17] (see the review [18]).

The geometry of the insulating post-array in the microchannel is one of the most important influencing factors in the performance of iDEP microfluidic devices. The first application of insulating post arrays to generate iDEP was presented by Cummings and Singh in 2003. In their studies, they investigated the effect of diamond and circular shape of insulating post-array on the generated iDEP [11]. Barbulovic-Nad et al. in 2006 used an oil droplet as an adjustable insulating structure to change the distance between the insulating structures and study how this affected to the dielectrophoresis [19]. Kwon et al. in 2007 presented a study focused on the improvement of the circular-post

geometry subject to electrokinetic (EK) and dielectrophoretic forces using a mathematical model. Their results indicated that when the longitudinal spacing between the posts was 0.6 times the post radius then the lateral-to-longitudinal force ratio was larger [20]. Nakano et al. in 2011 demonstrated iDEP-based manipulation of proteins using ellipsoidal and triangular shaped posts. Also their study presented an approximated numerical analysis of the electric field and the gradient of the electric field at the tip of the insulating posts [21]. Kim et al. in 2014 presented a simulation model to study the effect on protein concentration of circular and square post-arrays, both in-plane and out-of-plane [22]. Lalonde et al. in 2014 reported the effect of geometry on the trapping performance of iDEP. In their study, two different insulating-posts geometries (circle and diamond) were employed with a fixed spacing between them of 50 µm. The results indicated that the highest electric field gradient was achieved when diamond-posts were used [23].

Mohammadi et al. in 2015 presented a design that combined hydrodynamics and DC-iDEP flow for blood plasma separation using corrugated shape channel, which comprised 20 transversal distance from 16 µm to 127µm to study RBC trapping [24].

The aforementioned studies provide valuable insight into the effect of geometry on the DC-iDEP phenomena but they are focused on a particular geometry or a type of particles. On this basis, finding an efficient post-array geometry on DC-iDEP regardless the particle type, to minimize the required voltage as well as the Joule effect for the highest trapping condition is valuable particularly in those applications that require viable cell trapping. In this work, we propose a novel figure of merit to find an efficient design of the post-array distribution in a microfluidic channel for increasing the trapping value based on DC-iDEP. Furthermore, we provide a new relationship between geometrical parameters of micropost array including transversal distance between posts and radius of posts, not only to maximize the trapping value but also to minimize the required electric field and its effects.

The current study also investigates the optimum value of the post radius and the longitudinal distance between the posts for a given transversal distance between posts in a micropost array of microfluidic channel, to enhance the particle trapping using the direct current iDEP (DC-iDEP) method. To this aim, numerical modeling and experiments are performed to study the effect of these geometrical parameters. The electric field, the electric field gradient and the trapping condition are calculated in more than 300 models numerically. The results of the experiments confirm our predictions and numerical analysis. The result of this work can be a road map and new approach for the microfluidic designers (design, efficient insulator obstacles or post array) to achieve the maximum advantages of the DC-iDEP method.

This paper is organized as follows: Introduction in Section I, theoretical background, fabrication procedure and experimental setup are explained in Section II. Numerical models of DC-iDEP and experimental validation of the proposed device are presented in Section III. Concluding remarks are presented in Section IV.

## 2. Materials and methods

### 2.1. Theoretical background

When the DC electric field is applied in a channel, the ions from the electrolyte form an electric double layer (EDL) over the wall surface. The ions from the double layer are attracted to the negative electrode, producing an electroosmotic liquid flow (EO), described by the Helmholtz-Smulochowski equation according to which, theelectroosmotic velocity [16] is:

$$\vec{V}_{eo} = \mu_{eo}\vec{E} = \frac{\varepsilon_m \zeta_w}{\eta}\vec{E} \tag{1}$$

where $\vec{E}$ is the electric field, $\mu_{eo}$ is the electroosmotic mobility of the ionic fluid, $\zeta_w$ is the zeta potential of the wall of microchannel, $\eta$ is the viscosity and $\varepsilon_m$ is the permittivity of the fluid. The dielectrophoretic velocity plays an important role in the particle trapping. The DEP velocity is [25]:

$$\vec{V}_{DEP} = -\mu_{DEP}\nabla\vec{E}^2 \tag{2}$$

where $\vec{V}_{DEP}$ is the dielectrophoretic velocity and $\mu_{DEP}$ is the dielectrophoretic mobility which, in turn, can be expressed as [25]:

$$\mu_{DEP} = \frac{r^2\,\varepsilon_m f_{CM}}{3\eta} \tag{3}$$

where r is particle radius and, $f_{CM}$ is the Clausius-Mossotti factor. In DC-iDEP the frequency is zero, therefore the Clausius-Mossotti factor depends only on particle and medium conductivities [16]

$$f_{CM} = \frac{\sigma_P - \sigma_m}{\sigma_P + 2\sigma_m} \tag{4}$$

where $\sigma_P, \sigma_m$ are particle and medium conductivities. The Helmholtz-Smoluchowski equation describes also the electrophoretic EP experienced particle velocity [16]

$$\vec{V}_{ep} = \mu_{ep}\vec{E} = \frac{\varepsilon_m \zeta_p}{\eta}\vec{E} \tag{5}$$

Where $\zeta_p$ is the zeta potential of the particle.

The electrosmotic flow (from positive to negative electrode) is diminished by the electrophoretic flow (from negative to positive electrode), so three flows should be considered: electroosmotic (EO), electrophoretic (EP) and dielectrophoretic (DEP). Since the EO mobility is significant compared with EP mobility therefore, the EK flow is mainly dominated by Electroosmotic flow. The total velocity of the particles due to the combined effects of electroosmosis (EO), electrophoresis (EP) and dielectrophoresis (DEP) can be expressed as the superposition of a linear electrokinetic velocity $\vec{V}_{EK}$ (EOF + EP flow) and a nonlinear DEP flow:

$$\vec{V}_{tot} = \vec{V}_{EO} + \vec{V}_{EP} + \vec{V}_{DEP} = (\mu_{eo} - \mu_{ep})\vec{E} - \mu_{DEP}\nabla\vec{E}^2 \tag{6}$$

where $\vec{V}_{tot}$ is the total velocity and, $\mu_{ep}$ is electrophoretic mobility.

To achieve trapping of particles, DEP velocity must overcome EK velocity, since the direction of the EK flow, as observed experimentally, is from the positive electrode to the negative electrode in the microchannel (electroosmotic direction). Consequently, the net particle velocity along the electric field line is zero in the zone of trapping. Thus, the trapping DEP flow condition becomes as other authors reported [25-28]:

$$\frac{c\,\mu_{DEP}\nabla(\vec{E}.\vec{E}).\vec{E}}{\mu_{EK}\,\vec{E}.\vec{E}} > 1 \tag{7}$$

The $C$ is a correction factor that used to match the experiment with models.

Since we are not interested in the actual extension of the trapping zone, we do not include the DEP and EK mobility terms so the result is independent of the particle and medium properties. Therefore, the scalar field, defined by $T \equiv \frac{\nabla\vec{E}^2}{\vec{E}^2}.\vec{E}\,(V/_{m^2})$, is called trapping value and calculated to observe the effect of trapping for different geometries.

## 2.2. Chip fabrication and experimental setup

Soft-lithography technique is used to fabricate a 1-cm long and 1-mm wide PDMS microchannels with an embedded insulating post-array of 1-mm wide and 2-mm-long in the middle of the channel. Then the fabricated PDMS channel is bonded to a glass cover via an oxygen plasma treatment. A schematic top view of the microchannel used in this work is shown in Figure 1 (a). Several microchannels with different post radius (20, 70 and 150 µm) are fabricated. The transversal and longitudinal distances of the fabricated channels are then measured by confocal microscopy (Sensofar Plu neox, Sensofar -Tech, Terrassa, Spain).

Figure 1 (b) shows a contour plot of the 70-µm-radius post array. The average longitudinal distance is 50±3 µm and transversal distance is 30±3 µm are shown in Figure 1 (d-e). The post-diameter is 140±6 µm and the post height is 50±5 µm, as expected.

Each channel has been washed four times with DI water and filled with DI water 5 hours before the experiments. Afterwards, a 4-µl suspension (2.5% aqueous suspension) of polystyrene red dyed beads with a diameter of 6 µm and a concentration of $2.10 \times 10^8$ particles/ml (Warrington, Pennsylvania USA) are diluted in 16-µl of de-ionized water ($\varepsilon_r$=80.1; $\rho$=~20 kΩcm) [29] with a resulting PH of 6.5 and the sample is introduced in the channel inlet.

The zeta potential of the polystyrene beads suspension was measured by laser Doppler interferometry using a Malvern Zetamaster zeta potential analyzer, according to the results the zeta potential had to be < 0.05 mV. These results agree with values obtained by other authors such as Weiss et al. [30] who reported a DEP mobility of 1 um polystyrene beads of $-2\pm0.4 \times 10^{-8}$ cm$^4$/(V$^2$ s) or Ermolina and Morgan [31] who measured the zeta potential of 1-µm-radius latex particles in almost 0.04 mV and therefore the electrophoretic mobility of $2.84 \times 10^{-7}$cm$^2$V$^{-1}$s$^{-1}$.

Eventhough, for the used particles a combined zeta potential ($\zeta_w$- $\zeta_p$) mobility was measured experimentally by MicroPIV(Microscope Olympus IX71, Laser model NANO L135-15 PIV from Litron Lasers, Software INSIGHT 3G from TSI) and its value turns out to be $1.12 \times 10^{-4}$cm$^2$V$^{-1}$s$^{-1}$ $\pm$ $0.1 \times 10^{-4}$, in the order of magnitude of electroosmotic mobility in agreement with the previous studies.

To ensure about the negative charge of the surface of the PDMS microchannel, new PDMS microchannel are used in each experiment. In order to record the images and videos of the particle response, a digital camera (Tucsen ISH500,

5.0 M pixel,) is connected to a micro inspection lens system Optem zoom 125C (with a broad 12.5:1 zoom range) and a 20X objective.
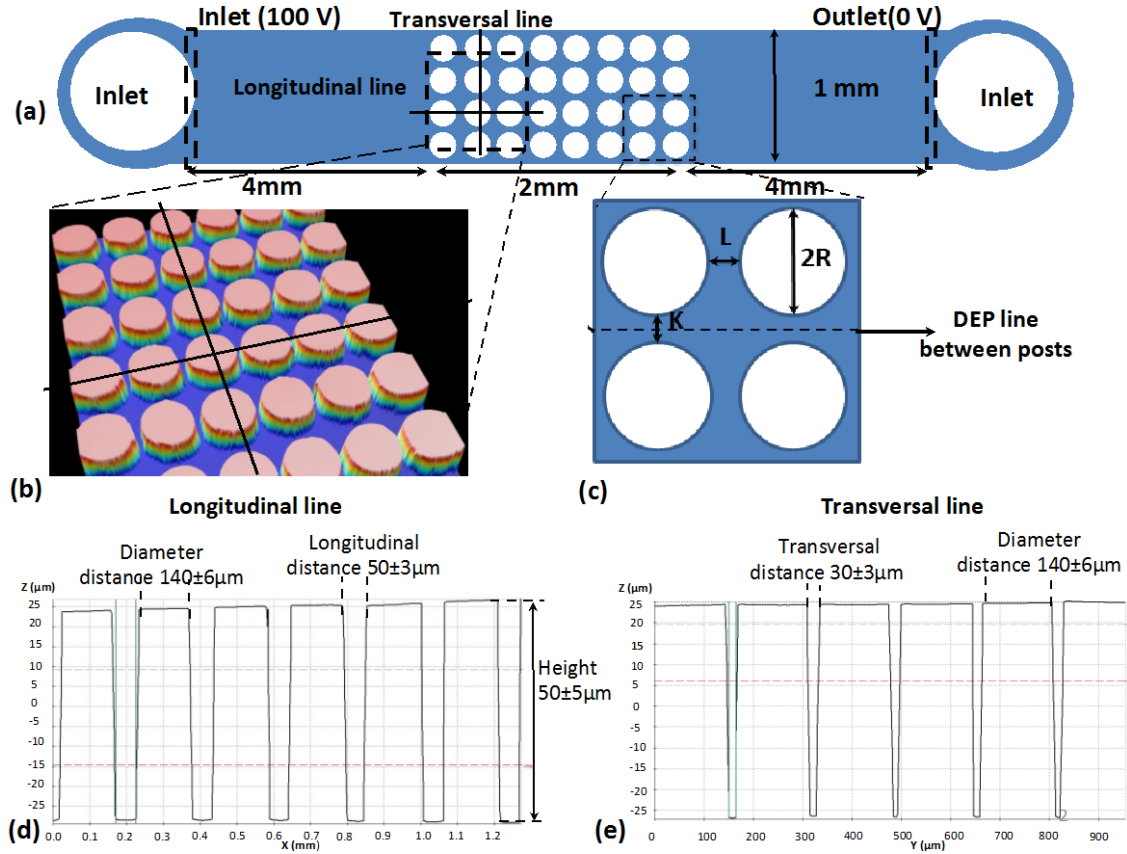


**Fig. 1** Schematics of the microchannels under test (b) Confocal image of a topography of the 70-μm-radius post-array (c)Variables of the design (d) Longitudinal distance and post height (e) Transversal distance cross-section

A DC voltage power supply (SF-9585 PASCO- California-USA) is utilized to generate the electric field. Two Platinum electrodes (Roland Consult-Germany) are placed in the inlet and outlet of the main channel to create the electric field. The microchannel and experimental setup is shown in Figure 2 (a, b).

## 3.   Results and discussion

The geometry of the insulating post-array in the microchannel has a main role in the proficiency of the iDEP micro device for the particle or cell trapping in many biochemical and biological applications. In fact, the presence of insulators in the microchannel distorts the electric field, producing gradients. From equation (6) it can be deduced that the dielectrophoretic force exerted on particles in a medium is proportional to the gradient of squared electric field; therefore, it is concluded that the geometry of insulators directly influences on the electric field distributions and consequently the performance of iDEP micro devices.

In order to analyze the geometrical parameters of microarray on the distribution of the electric field and the gradient of the squared electric field, the numerical code from Electric current module of COMSOL Multiphysics commercial software is used.
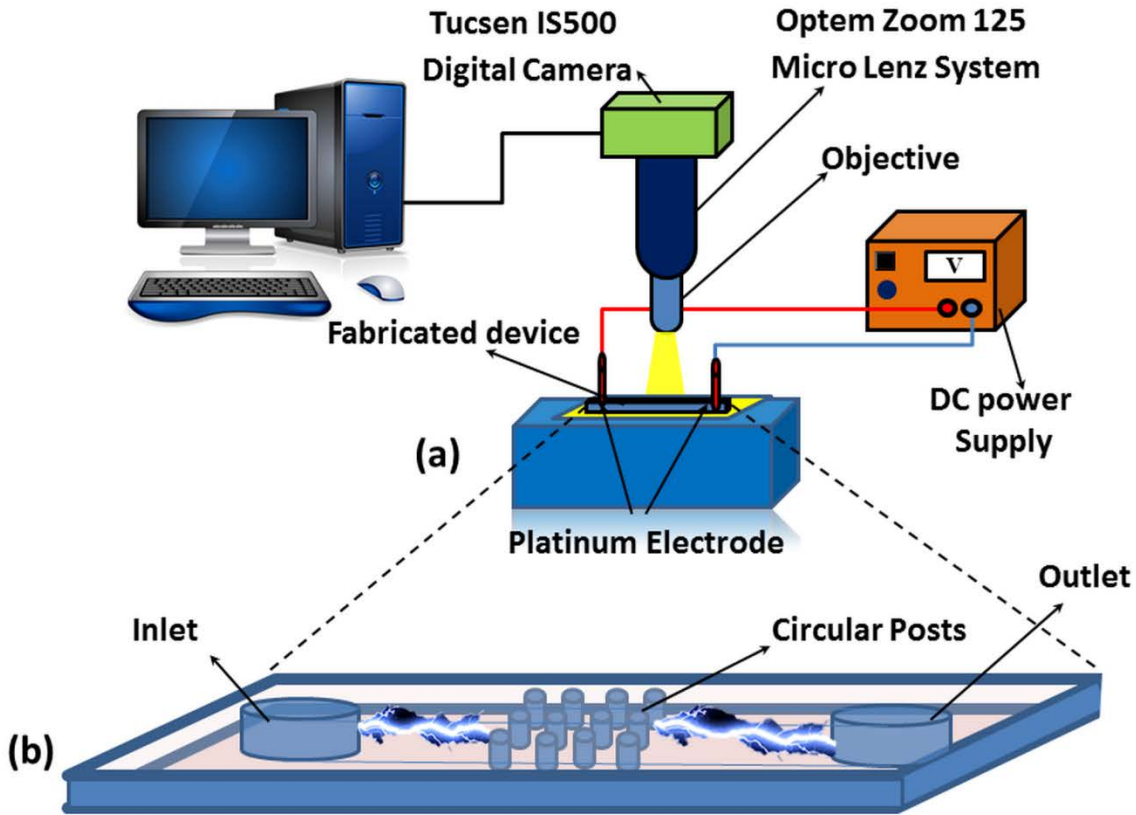


**Fig. 2** (a) Experimental set-up and (b) DC iDEP microdevice schematic picture

The parameters that define the geometry of the post array are shown in Figure 1 (a and c), where R is the radius of the post, K is the transversal distance between posts and L is the longitudinal distance between two adjacent posts.

A 2D numerical model of a 1-cm long and 1-mm wide microchannel, with a 2-mm long and 1-mm wide array of circular posts located in the middle of the microchannel is defined. The electric potential difference of 100 V is applied between channel inlet and outlet as a boundary condition in COMSOL. The values of R and K are varied, and 300 different models are created and simulated.

In order to obtain results independent from the particle and medium properties, the quantity of trapping value, $T \equiv \frac{\nabla \vec{E}^2}{\vec{E}^2} \vec{E}$ , has been calculated in all simulations. T is a particle- and medium-independent scalar field that accounts for the trapping capability of each point. Since we are interested to study the dependency of individual geometrical parameters on the distribution of electric field, when one of the parameters is varied, the other parameters remain

8

unchanged. The following analysis elucidate more the influence of micro post-array geometry on the electric field distribution and consequently particle trapping.
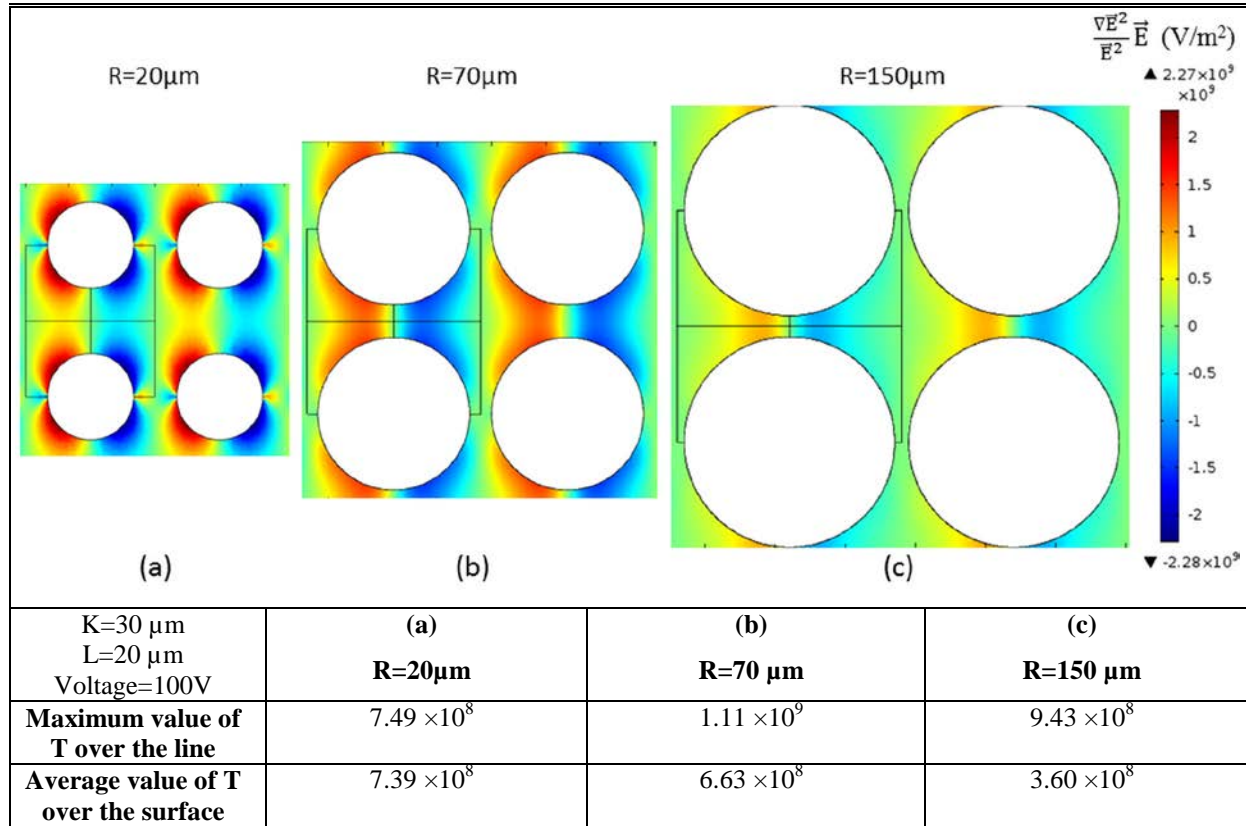
Grid independency for the trapping value simulation was checked to ensure that the solutions were independent of the number of elements, see supplementary information for more details. (Online Resource 1).

### 3.1. Effect of post geometry on the distribution of electric field

Saucedo-Espinosa et al [26] in their study about the effect of particle size and shape on the particle trapping post arrays pointed out that the analysis of the maximum trapping value on the line between two posts could help to establish a geometry of post array that unambiguously creates trapping. To deepen in this assumption, three circular posts with the radius of 20 µm, 70 µm, and 150 µm have been selected to make a preliminary study of the iDEP trapping with the purpose of finding a figure of merit that can be optimized. The transversal distance (K) is fixed to 30 µm and L is fixed to 20 µm. The average trapping value (T) over the surface between the posts, and the maximum trapping value (T) on the line between the posts are shown for each geometry in Table 1, in order to determine if it is possible to optimize any of these parameters.

In case (a), R =20 µm, the higher values of T, as it can be seen in Table 1, are mainly concentrated near the posts but are lower on the line between the two posts.

Table 1. Different numerical modeling of trapping value by different R and constant K, L and voltage



| K=30 µm<br>L=20 µm<br>Voltage=100V | (a)<br><br>R=20µm | (b)<br><br>R=70 µm | (c)<br><br>R=150 µm |
|---|---|---|---|
| Maximum value of T over the line | $7.49 \times 10^8$ | $1.11 \times 10^9$ | $9.43 \times 10^8$ |
| Average value of T over the surface | $7.39 \times 10^8$ | $6.63 \times 10^8$ | $3.60 \times 10^8$ |

While case (b), R = 70 µm, presents a more evenly distributed electric field gradient in comparison with R=20 µm. The maximum trapping value (T) on the plotted line is $1.11x10^9$, while in case (a) this value is $7.49x10^8$. This means that microparticle trapping occurs at a lower applied voltage for a radius of 70 µm. Note that the average trapping value (T) over the surface in case (a) is greater than in case (b). This is due to the fact that when the post radius is smaller, a greater electric field gradient is obtained. Therefore, the average value of trapping (T) over the surface will not be a correct criterion for the comparison of microparticle trapping because it is not optimizable. Moreover, it is observed in trapping experiments that effective filtering occurs when trapping takes place near (or at) the center of the channel. The average of the trapping value may have little sense as a figure of merit if trapping takes place mainly at zones far from the center of the channel. Aside from being optimizable, the maximum value of T in the central line of the channel has the advantage that reflects the existence of a trapping zone that, even if it is not extensive, can achieve effective filtering. We claim that optimization using this figure of merit should lead to behavior qualitatively similar to the one observed experimentally and can be useful as a guide to improve microfiltering designs because of its simplicity and ease of calculation even if it is not proved that it is the best possible figure of merit.

As shown in case (c), where the radius of the posts is 150 µm, T is smaller in comparison with case (b). The maximum trapping value (T) along the middle line is $9.43 x10^8$ which is smaller than in case (b). This shows that there will be an optimum value for the radius of the posts., The average of trapping value (T) over the surface in this case is about $3.60 x10^8$ which is smaller than the two previous cases. It can be seen that as the radius of the posts decreases, keeping transversal and longitudinal distances constant, the T gets more intense and is mainly concentrated near the posts (see maximum of scale bar of figures $2.28\times10^9$ (V/m2)) also, the trapping zone shifts to the center of the posts by increasing post radius

### 3.2 Experimental validation

To experimentally observe the effect of insulating post-radius on trapping performance, a run of three different PDMS micro channels for each of the different radius post-arrays (R=20, 70, 150 µm) with the transversal distance equal to 30 µm and the longitudinal distance of 50 µm were tested. The aqueous suspension of 6-µm-diameter polystyrene microsphere particles diluted (1:4) in deionized water with a resulting PH of 6.5. Later this is introduced into the channels to carry out the trapping experiment. Then, DC voltages of 200, 350 and 500 V are applied to observe particle trapping for each post-array geometry.

The DEP mobility, as presented in equation (1) for current polystyrene particles, is$-1.06 \times 10^{-18} m^4/(V^2 s)$. The negative sign of this value is due to the negative Clausius-Mossotti factor which is assumed as $-0.5$ for these particles under DC electric fields [23]. Figure 3 shows one example of the performance of trapping for each geometry 30 s after the electric field has been applied.

Changing the geometry of the insulator post-array results in a change of the electric field distribution. This has an immediate effect on EK velocity, but also, through the gradient of the squared electric field, affects DEP velocity. Particle trapping can be achieved when the DEP contribution to particle velocity is larger than the EK contribution.

The performance of microparticle trapping of an insulating post-array with R=20 µm is shown in Figures 3 (a-c). The experimental pictures present particle trapping confined on the surface of the post and mainly concentrated near the posts. There is no particle trapping present in the separation zone between the posts. Thus, in order to achieve efficient particle separation a high DC voltage is required, see Supplementary movie (Online Resource 2). (R=20 µm at 200, 350, 500V). Figures 3 (d-f) demonstrate efficient particle trapping of an insulating post-array with R=70 µm starting at 200 V, see Supplementary movie (Online Resource 3). (R=70 µm at 200, 350, 500V). The observed performance implies that the maximum of the trapping value (T) along the line between the posts is a better figure of merit than the average of T over the surface.
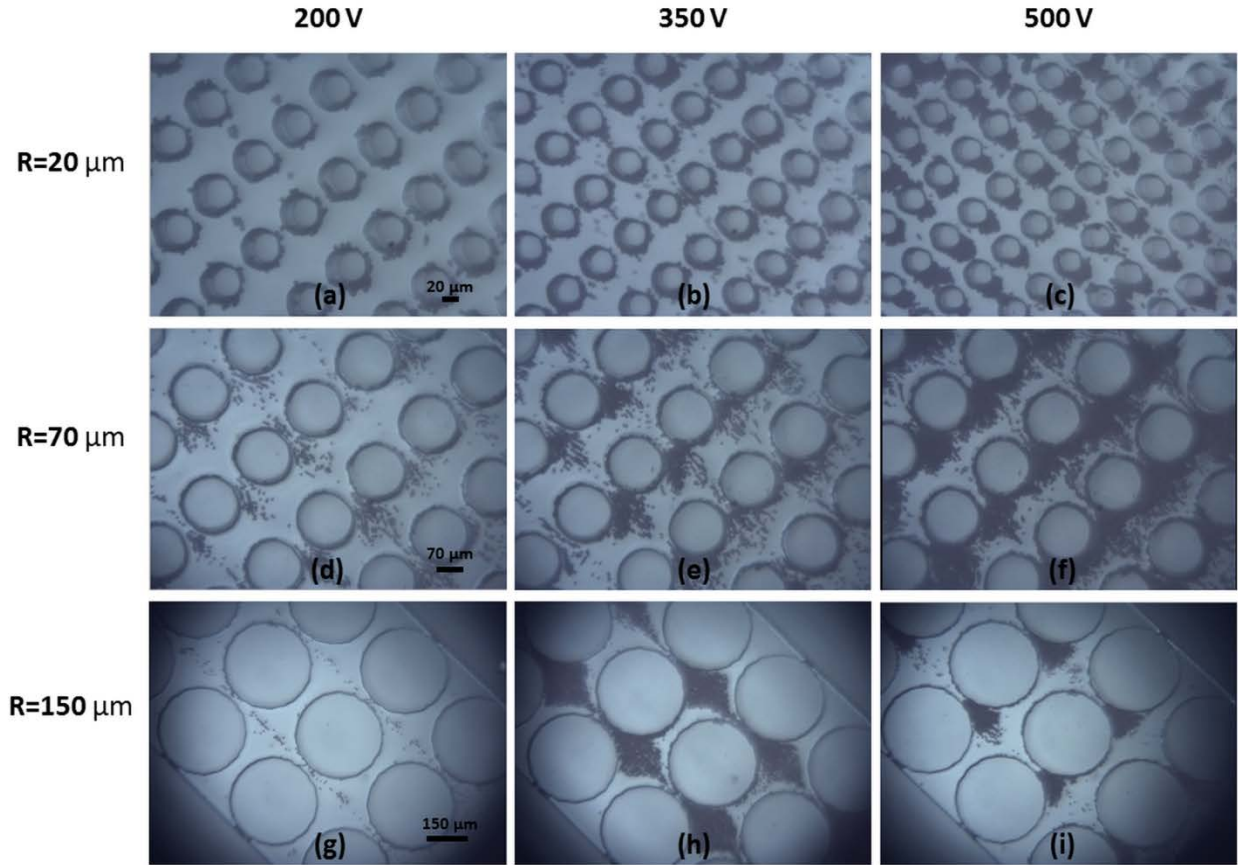


**Fig. 3** Polystyrene beads' trapping pictures 30 s after applying the DC voltage of 200 V, 350 V and 500 V to a post-array of radius (a-c) 20 µm (d-f) 70 µm, (g-i) 150 µm.

An example of particle trapping for R=150 µm is depicted in Figures 3 (g-i). Streaming flow appears for 200 V and 350 V and particle trapping is observed only for 500 V, see Supplementary movie (Online Resource 4). (R=150 µm at 200, 350, 500V). The experimental results indicate that the DEP velocity is greater than the EK velocity in an insulating post-array with R=70 µm, in which a significant number of particles have been separated with a lower voltage in comparison with R=20 and 150 µm. In addition, experimental results confirm the predicted numerical results that as the radius of the posts decreases, keeping transversal and longitudinal distances constant, trapping of particles gets more intense and is mainly concentrated near the posts.

11

### 3.3  Optimum radius of the post

In order to find the optimum radius of the post, the maximum value of trapping (T) on the line between two adjacent posts has been calculated in 300 models of micropost arrays. In these models, the value of R varies between 10 µm to 150 µm while the values of the transversal distance (K) changes between 10 µm to 60 µm. The value of L has been fixed to 20 µm and a voltage of 100 V is applied on a 1-cm long channel for all models.
Figure 4 shows the result of the numerical simulation for the variation of the trapping value (T) on the line between the posts according to the posts radius for different transversal distance (K), to find the optimum R. The predicted results indicate that there is a specific radius of posts for each K, which presents the maximum value of the trapping value (T). This post radius is considered as the optimum post radius for the particle trapping. Furthermore, it can be highlighted that for all the post radius, the trapping value (T) increases significantly with decreasing the transversal distance from 60 µm to 10 µm.
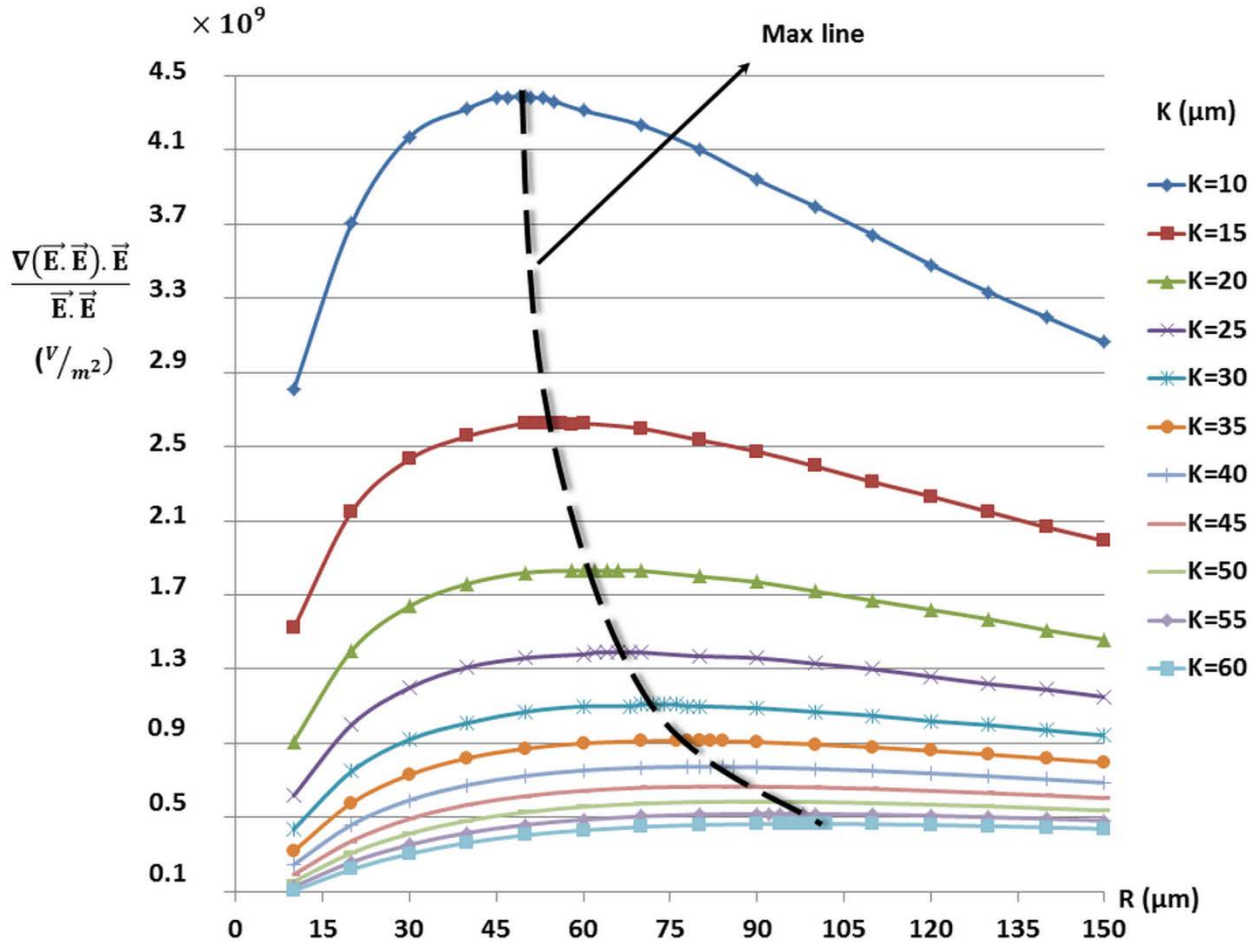


**Fig. 4** Trapping versus radius of the posts for different K

According to the predicted results (Figure 4), the relationship between the optimum radius R and the transversal distance K can be achieved as follows.

$$R_{opt} = K + 40 \pm 1 \mu m \tag{8}$$

This equation is a global equation, which is independent of particle and medium properties.

All optimum values of post radius (R) and the maximum trapping value (T) for each K (transversal distance varies between 10 and 60 µm) are presented in Table 2. In addition, this table shows the evolution of the trapping value T including both minimum and maximum value for a given K. Last row shows that the increase in the trapping value T from the non-optimized geometry to the optimum post radius can vary between 56% and 341% when the transversal distance varies from 10 to 60 µm.

Table 2.Trapping value and optimum R for each K

| K (µm) | 10 | 15 | 20 | 25 | 30 | 35 | 40 | 45 | 50 | 55 | 60 |
|---|---|---|---|---|---|---|---|---|---|---|---|
| Optimum R (µm) | 50 | 56 | 60 | 66 | 70 | 76 | 80 | 86 | 90 | 95 | 100 |
| The maximum of $\frac{\Delta \vec{E}^2}{\vec{E}^2} \vec{E} \times 10^9$ | 4.39 | 2.63 | 1.83 | 1.39 | 1.11 | 0.914 | 0.774 | 0.668 | 0.586` | 0.520 | 0.467 |
| The minimum of $\frac{\Delta \vec{E}^2}{\vec{E}^2} \vec{E} \times 10^9$ | 2.81 | 1.52 | 0.91 | 0.618 | 0.437 | 0.319 | 0.246 | 0.193 | 0.155 | 0.127 | 0.106 |
| Percentage of increase (%) | 56.4 | 72.8 | 101 | 125 | 154 | 187 | 215 | 246 | 278 | 309 | 341 |

### 3.4  Effect of longitudinal distance (L)

In this section, the effect of the longitudinal distance between posts (L) has been studied for different K and R. The modeling result shows the effect of L on the trapping value (T), which is rather weak with monotonic behavior when R is smaller than 70 µm, however, when L is increased T value can be enhanced up to 0.05 %, when R is bigger than 70 µm. The effect of L on the trapping value (T) for optimum R and different K is plotted in Figure 5.

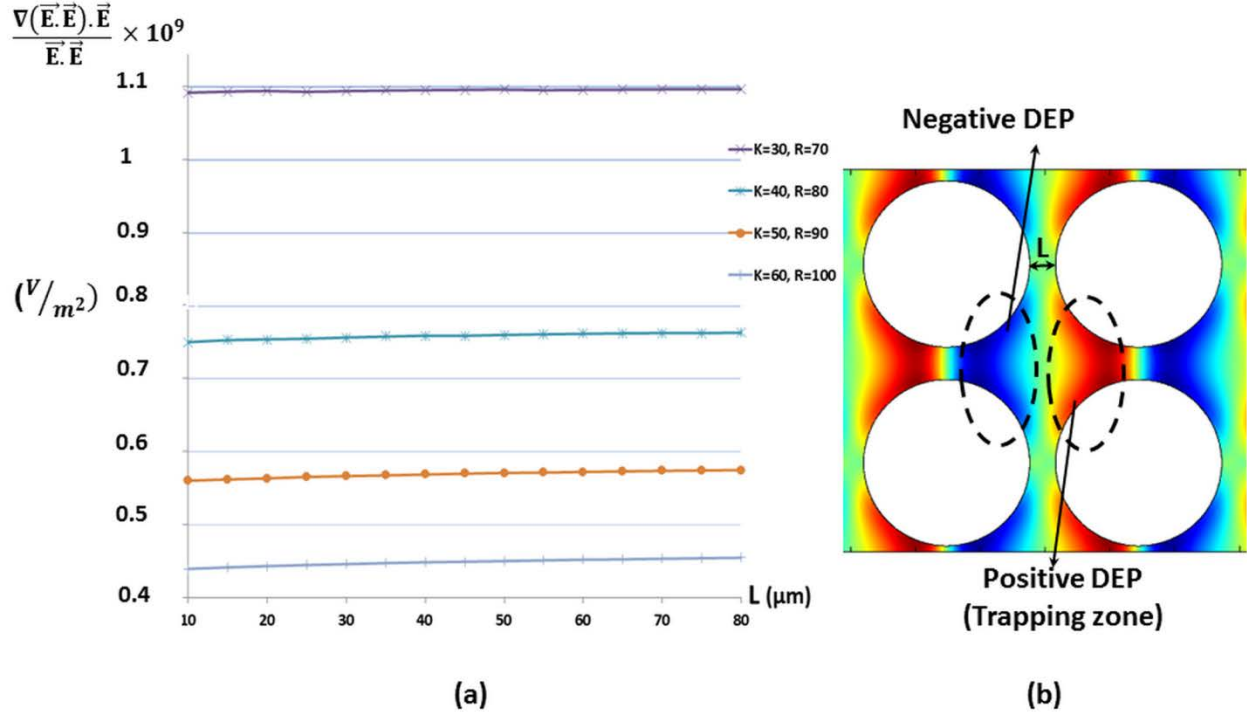$$\frac{\nabla(\vec{E}.\vec{E}).\vec{E}}{\vec{E}.\vec{E}} \times 10^9$$

Fig. 5 L effect on value of trapping for different K

These results can be explained due to overlapping effect of the negative DEP zone from the previous post column on the positive DEP zone of the next post column. This overlapping effect disappears when L is increased and therefore the trapping value is enhanced, see Figure 5 (b).

In summary, the obtained results are independent of particle and medium properties and can be applied to all particles and mediums. The numerical results show that the modification of geometrical parameters of the post-array can significantly reduce the required electric potential to achieve effective enrichment and particle trapping. Moreover, the set of experimental results validates the numerical simulation results which show that for constant transversal distance between posts (i.e 30 µm) there is an optimum radius of the post (i.e. for k= 30 µm isR=70 µm) to achieve the maximum trapping value.

Recently, the performance of two different insulating post-array geometries including circle and diamond post shape have been studied [23]. Further more, circular and square post-arrays have been used in-plane and out-of-plane for protein concentration [22] and ellipse and triangle-shaped posts have been used for manipulation of proteins [21] None of these previous studies were based on an independent geometrically optimized design.

The use of the most efficient post-array arrangement derived from obtained relationship (equation 8), opens the possibility to improve the previous investigations or implement of future study not only to minimize the required voltage to achieve trapping, but also minimizing the Joule effect.

## 3    Concluding remarks

To ensure an efficient trapping design, the geometry of the insulating post-array in the microchannel is one of the most important factors in the performance of iDEP microfluidic devices. Cummings and Singh already meantioned the importance of the post array distribution on the efficiency of iDEP trapping in 2003 [11], later Barbulovic-Nad et al. in 2006 proposed an active method using oil droplets to adjust the insulating structure to be able to modify the trapping efficiency [19]. The idea of proving the microfluidics designers with simple equations or relationships between post array parameters started to be explored by Kwon et al. in 2007 who proposed that when the longitudinal spacing between the posts was 0.6 times the post radius then the lateral-to-longitudinal force ratio was larger [20], this study ensure a maximum in area between posts, but it could be that the maximum trapping value occurred near the post walls without a guarantee that the trapping path was completely blocked. Saucedo et al. in their recent study [26] already introduce the idea that to achieve filtration/trapping, trapping has to be guarantee in the line between the two posts.

This paper presents a strategy to find the efficient geometry of the post-array distribution in DC-iDEP microdevices that maximizes the trapping condition, while minimizing the required voltage, similar footprint and the channel thickness. COMSOL Multiphysics software has been used to perform a parametric characterization of the geometric parameters of the post-array based on a new proposed figure of merit (the maximum of trapping condition along the central line of the transversal distance between posts, T). A high value of this figure of merit will denote the existence of trapping zones close to the center of the channel and therefore will be an indicator of effective filtering. It is reasonable to expect that optimization of this figure of merit will reproduce, at least qualitatively, real behavior. More than 300 different post-array geometric models with transversal distance between posts varying from 10 to 60 µm have been investigated. The results of the geometrical characterization show that the efficient micropost array can reduce the required electric field to achieve an effective trapping and, therefore, avoid the negative effects of Joule heating. The results indicate that there is a specific radius of posts (R) for each transversal distance (K) which can enhance the trapping condition between (56.1% to 341%) compared to the initial non-optimized design. This behavior has been captured through a proposed relationship between the transversal distance between posts (K) and the optimum posts radius (R). Moreover, the obtained results show that the effect of increasing of the longitudinal distance (L) on trapping value is insignificant when K is smaller than 30 µm but trapping value is enhanced (0.05%) when K is more than 30 µm. The numerical results are validated using microchannels with embedded post-arrays, manufactured in Polydimetilsiloxane (PDMS) to trap polystyrene beads. Experiments confirm a higher trapping for those micropost geometries closer to the optimal value determined by numerical simulation, reinforcing the idea that our figure of merit is useful at least to predict qualitatively the performance of a microfiltering device. The proposed figure of merit depends only on the geometry of the micropost array and show that the geometrical characterization results can be used not only to reduce the required electric field to achieve effective trapping of any kind of particle, but also avoid the negative effects of Joule heating specially when dealing with biological cells. It also has the advantage that is easy to calculate and has a clear physical interpretation. Therefore, the use of the derived equation can be an important milestone for a wider use of DC-iDEP devices for trapping viable cells.

**AUTHOR INFORMATION**
* Corresponding Author: Address: MicroTech Laboratory, Department of Mechanical Engineering, Technical University of Catalonia, Terrassa 08222, Spain. E-mail. Jasmina.casals@upc.edu

**References**

[1]     Whitesides G (2014) The lab finally comes to the chip. Lab Chip 14: 3125–3126

[2]     Lenshof A, Laurell T (2010) Continuous separation of cells and particles in microfluidic systems. Chem. Soc. Rev 39 ( 3): 1203–17

[3]     Sajeesh P, Sen AK (2014)Particle separation and sorting in microfluidic devices: a review. Microfluid. Nanofluidics 17 (1): 1–52

[4]     Clague D, Wheeler E (2001) Dielectrophoretic manipulation of macromolecules: The electric field. Phys. Rev. E 64 (2): 026605

[5]     Gascoyne P, Vykoukal J (2002) Particle separation by dielectrophoresis. Electrophoresis 23: 1973–1983

[6]     Cetin B, Kang Y, Wu Z, Li D (2009) Continuous particle separation by size via AC-dielectrophoresis using a lab-on-a-chip device with 3-D electrodes. Electrophoresis 30 (5): 766–772

[7]     Qian C, Huang H, Chen L, Li X, Ge Z, Chen T, Yang Z, Sun L (2014) Dielectrophoresis for Bioparticle Manipulation. Int. J. Mol. Sci. 15 (10): 18281–18309

[8]     Jubery TZ, Srivastava SK, Dutta P (2014) Dielectrophoretic separation of bioparticles in microdevices: a review. Electrophoresis 35 (5):691–713

[9]     Braff WA, Pignier A, Buie C R (2012) High sensitivity three-dimensional insulator-based dielectrophoresis. Lab Chip 12 (7): 1327–31

[10]    Regtmeier J, Eichhorn R, Viefhues M, Bogunovic L, Anselmetti D (2011) Electrodeless dielectrophoresis for bioanalysis: theory, devices and applications. Electrophoresis 32 (17): 2253–73

[11]    Cummings EB, Singh AK (2003) Dielectrophoresis in Microchips Containing Arrays of Insulating Posts Theoretical and Experimental Results. Anal. Chem 75(18): 4724–4731

[12]    Srivastava SK, Baylon-Cardiel JL, Lapizco-Encinas BH, Minerick AR (2011) A continuous DC-insulator dielectrophoretic sorter of microparticles. J. Chromatogr. A 1218 (13): 1780–9

[13]    Lapizco-encinas BH, Simmons BA, Cummings EB, FintschenkoY (2004)"Dielectrophoretic concentration and separation of live and dead bacteria in an array of insulators. Anal. Chem. 76( 6): 1571–9

[14]    Cho YK, Kim S, Lee K, Park C, Lee JG., Ko C (2009) Bacteria concentration using a membrane type insulator-based dielectrophoresis in a plastic chip. Electrophoresis 30 (18): 3153–9

[15] Kang Y, Li D, Kalams SA, Eid JE (2008) DC-Dielectrophoretic separation of biological cells by size. Biomed. Microdevices10 (2): 243–9

[16] Srivastava SK, Artemiou A, Minerick AR (201) Direct current insulator-based dielectrophoretic characterization of erythrocytes: ABO-Rh human blood typing. Electrophoresis 32 (18): 2530–40

[17] Jones PV, Staton SJR, Hayes MA (2011) Blood cell capture in a sawtooth dielectrophoretic microchannel. Anal. Bioanal. Chem 401 ( 7): 2103–11

[18] Srivastava SZ, Gencoglu A, Minerick AR (2011) DC insulator dielectrophoretic applications in microdevice technology: a review. Anal. Bioanal. Chem 399 (1): 301–21

[19] Barbulovic-Nad I, Xuan X, Lee JSH, Li D (2006).DC-dielectrophoretic separation of microparticles using an oil droplet obstacle. Lab Chip 6 ( 2): 274–9

[20] Kwon JS, Maeng JS, Chun MS, Song S (2007) Improvement of microchannel geometry subject to electrokinesis and dielectrophoresis using numerical simulations. Microfluid. Nanofluidics 5 (1): 23–31

[21] Nakano A,. Chao TC, Camacho-Alanis F, Ros A (2011) Immunoglobulin G and bovine serum albumin streaming dielectrophoresis in a microfluidic device. Electrophoresis 32 (17): 2314–22

[22] Kim D, Shim J, Chuang HS, Kim KC (2014) Effect of array and shape of insulating posts on proteins focusing by direct current dielectrophoresis. J. Mech. Sci. Technol. 28(7): 2629–2636

[23] Lalonde A, Gencoglu A, Romero-Creel MF, Koppula KS, Lapizco-Encinas BH (2014) Effect of insulating posts geometry on particle manipulation in insulator based dielectrophoretic devices. J. Chromatogr. A 1344: 99–108

[24] Mohammadi M, Madadi H, Casals-Terré J, Sellarès J (2015) Hydrodynamic and direct-current insulator-based dielectrophoresis (H-DC-iDEP) microfluidic blood plasma separation. Anal. Bioanal. Chem 407 (16): 4733–4744

[25] Baylon-Cardiel JL, Lapizco-Encinas BH, Reyes-Betanzo C, Chávez-Santoscoy AV, Martínez-Chapa SO, (2009) Prediction of trapping zones in an insulator-based dielectrophoretic device. Lab Chip 9 (20): 2896–901

[26] Saucedo-Espinosa MA, Lapizco-Encinas BH (2015) Experimental and theoretical study of dielectrophoretic particle trapping in arrays of insulating structures: Effect of particle size and shape. Electrophoresis 36: 1086-1097

[27] Kang KH, Xuan X, Kang Y, Li D (2006) Effects of dc-dielectrophoretic force on particle trajectories in microchannels. J. Appl. Phys 99: 064702-064708

[28] Zhu JJ, Tzeng TRJ, Hu GQ, Xuan XC (2009) DC dielectrophoretic focusing of particles in a serpentine microchannel. Microfluid. Nanofluid 7: 751-756

[29] Mescher M, Brinkman AGM, Bosma D, Klootwijk JH, Sudhölter EJR, Smet LCPMD(2014) Influence of conductivity and dielectric constant of water-Dioxane mixtures on the electrical response of SiNW-based FETs. Sensors (Switzerland) 14: 2350–2361

[30] Weiss NG, Jones PV, Mahanti P, Chen KP, Taylor TJ, Hayes MA (2011) Dielectrophoretic mobility determination in DC insulator-based dielectrophoresis. Electrophoresis 32: 2292-2297

[31]     Ermolina I, Morgan H (2005)The electrokinetic properties of latex particles: Comparison of electrophoresis and dielectrophoresis. J Colloid Interface Sci 285: 419–428